Final Report on the CIPM Air Speed Key Comparison (CCM.FF-K3)

Octorber, 2007

Yoshiya Terao[1], Mijndert van der Beek[2],
T. T. Yeh[3] and Harald Müller[4]

[1] NMIJ, AIST, Japan
[2] NMi VSL Flow, Netherlands
[3] NIST, USA
[4] PTB, Germany

1. Introduction

This key comparison, CCM.FF-K3 has been undertaken by CCM Working Group for Fluid Flow for the purpose of determining the degree of equivalence of the national standards for air speed measurement among the participating national metrology institutes. Four national metrology institutes have tested a transfer standard and compare their calibration results at the air speeds of 2 m/s and 20 m/s.

The participants are NIST (the United States), NMi (the Netherlands), NMIJ/AIST (Japan) and PTB (Germany). NMIJ/AIST has been assigned as the pilot laboratory.

This Draft B report was prepared in accordance with the Guidelines for CIPM Key Comparisons (the “Guidelines”) [CIPM 1999].

2. Participants and test schedule

The participating institutes and their actual testing dates are listed in Table 1.

Table 1. Participants and test schedule.

#	Participating institute (Country)	Test Dates	Remarks
1	NMIJ/AIST (Japan)	April 18, 2005 to April 27	
2	NMi (Netherlands)	May 12 to June 13	
3	NIST (US)	June 28 to July 22	Shock sensor #2 and #3 had been activated on arrival.
4	NMIJ/AIST (Japan)	July 28 to August 26	
5	PTB (Germany)	September 9 to November 11	
6	NMIJ/AIST (Japan)	November 18 to December 9	

3. Transfer Standard

In this key comparison, an ultrasonic anemometer was circulated as a transfer standard.

The ultrasonic anemometer is manufactured by KAIJO SONIC CORPORAITION. The probe has three pairs of ultrasonic transducers, and measures the three-dimensional velocity vector derived from the propagation time of the ultrasonic waves between each pair of transducers. The signal processing unit provides a scalar value of the air speed, V_{m}, which is given by,

$$V_{\mathrm{m}} = \sqrt{V_{\mathrm{x}}^2 + V_{\mathrm{y}}^2 + V_{\mathrm{z}}^2} \qquad (1)$$

where V_x, V_y and V_z denote the components of the three-dimensional velocity vector. This signal processor also gives the time averaged air speed, $\overline{V_m}$.

Photo 3-1 shows the probe set to be calibrated in the test section of the wind tunnel at NMIJ.

Photo 3- 1 Probe of the ultrasonic anemometer

Note: A vane anemometer was also circulated along with the ultrasonic anemometer. However the description or the measurement result of this anemometer is not presented here because the anemometer did not serve as a transfer standard in this key comparison.

(3) Condition of the TS package during the KC

The transfer standard (TS) was shipped in a dedicated transportation box that measures 1020 mm (width) × 420 mm (height) × 545 mm (depth) and weighs 45 kg including the TS. Three shock sensors were contained in the box to detect unexpected shock or impact during transportation.

When the transfer package arrived at NIST from NMi, Two of the shock sensors, which were sensitive to the vertical acceleration, were found activated although no visual or functional damage was observed on the transfer standards.

4. Calibration results

(1) Calibration results reported by the participating institutes

At each participating institute, the ratios of the laboratory's reference air speed (V_{ref}) to the time averaged air speed $\overline{V_m}$ were obtained at 2 m/s and 20 m/s and reported with their uncertainty. The averaging time was 60 s. In this report the calibration result is represented by

$$x_{i,} = V_{ref} / \overline{V_m} \qquad (2)$$

where subscript *i* denotes the participating institute.

(2) Reproducibility of the TS observed at NMIJ

Fig.4-1 shows the calibration results of the ultrasonic anemometer at NMIJ obtained before starting the circulation, when it returned from NIST and after the end of the circulation. This figure indicates that the anemometer was very stable both at 2 m/s and 20 m/s.

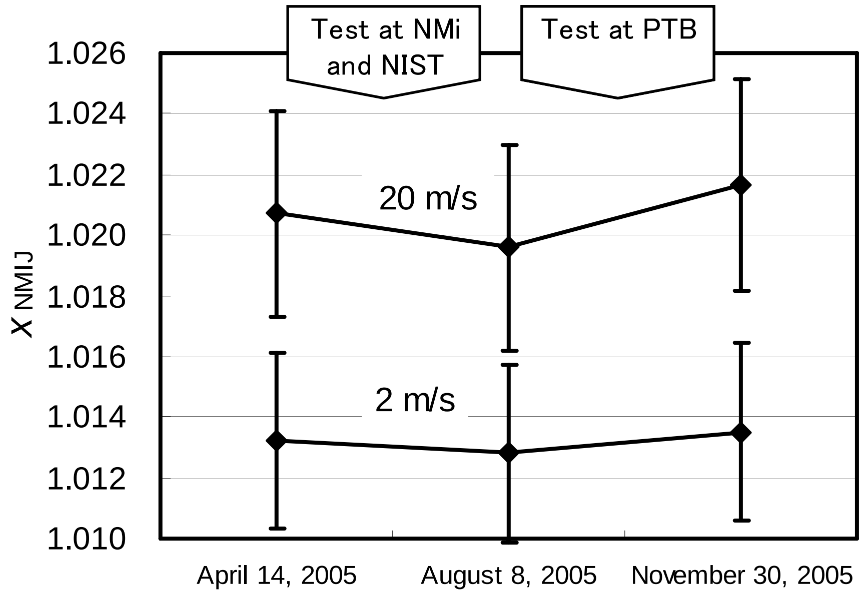

Fig. 4-1 Result of reproducibility test of the ultrasonic anemometer

(3) Calibration results of the participating institutes

The calibration results reported by the participating institutes are listed in Table 4-1. Among the three sets of date at NMIJ shown in Fig. 4-1, the result obtained on August 8, 2005 was chosen.

Table 4-1 Calibration results reported by the participating institutes
$U(x_i)$ is an expanded uncertainty with coverage factor (k) of 2.

i	20 m/s		2 m/s	
	x_i	$U(x_i)$	x_i	$U(x_i)$
NMi	1.0064	0.0052	0.9993	0.0052
NIST	1.0080	0.0061	1.0090	0.0055
NMIJ	1.0128	0.0029	1.0196	0.0034
PTB	1.0120	0.0030	1.0270	0.0050

5. Determination of KCRV

(1) Weighted mean and chi-squared test (Procedure A)

The calibration results of the transfer standard were analyzed according to the procedure A of the Cox method [Cox 2002]. Table 5-1 shows the weighted mean of the calibration results and the result of the chi-squared test.

At 20 m/s, the chi-squared test did not fail and the weighted mean has been accepted as the KCRV (x_{ref}). When estimating the uncertainty of the KCRV, uncertainty due to instability of the transfer standard was combined with $u(y)$ by root-sum-square method. The additional standard uncertainty was 0.00075, which corresponds to 0.015 m/s.

$$x_{ref} = 1.0113, \quad U(x_{ref}) = 0.0024\ (k = 2), \quad \text{at 20 m/s} \qquad (3)$$

The calibration results from the participating institutes and the KCRV and their expanded uncertainties at 20 m/s are plotted in Fig. 5-1.

Table 5-1 Weighted mean and chi-squared test

	20 m/s	2 m/s
Weighted mean y	1.0113	1.0155
Standard deviation associated with y $u(y)$	0.0009	0.0011
Observed chi-squared value χ^2_{obs}	6.0	71
Degree of freedom $\nu = N - 1$	3	3
$\Pr\{\chi^2(\nu) > \chi^2_{obs}\}$	0.11 (> 0.05)	0.00 (< 0.05)
Result of chi-squared test	Not failed	Failed

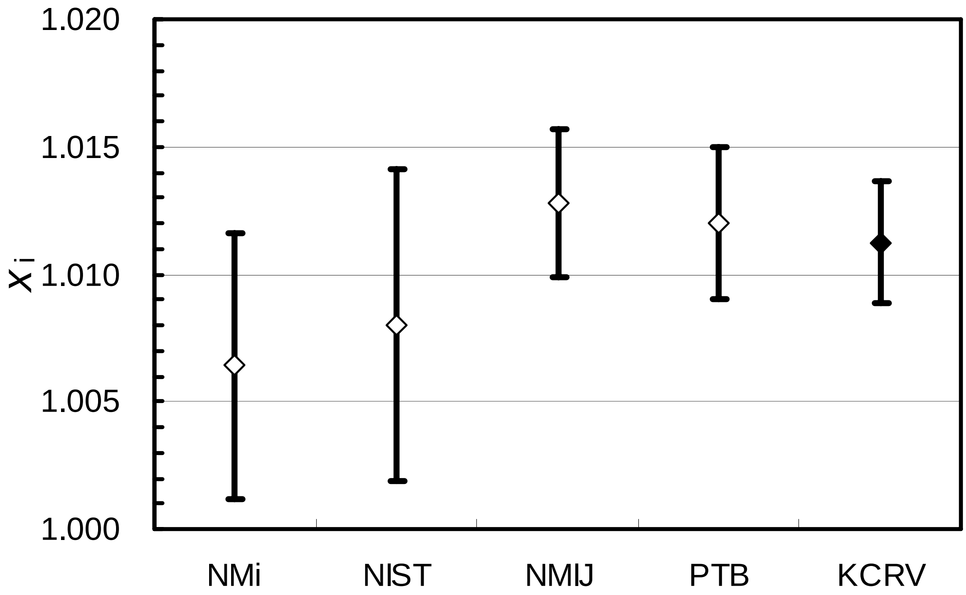

Fig. 5-1 Result of the key comparison (20 m/s)

6. Estimation of the median as KCRV (Procedure B) at 2 m/s

At 2 m/s, the chi-squared test failed thus the procedure B of the Cox method was performed. As a result of 10^6 of Monte Carlo trials, it is determined that the KCRV at 2 m/s is 1.0143, which is very close to the weighted mean. At this speed, the mathematically obtained standard uncertainty of the KCRV was 0.0017 and the additional standard uncertainty due to instability of the transfer standard (0.015 m/s) was 0.0075. These two uncertainty sources were combined by root-sum-square method and the expanded uncertainty (k = 2) of the KCRV was obtained as 0.0154.

$$x_{ref} = 1.0143, \quad U(x_{ref}) = 0.0154 \ (k = 2), \quad \text{at 2 m/s} \qquad (4)$$

The calibration results from the participating institutes and the KCRV and their expanded uncertainties at 2 m/s are plotted in Fig. 6-1.

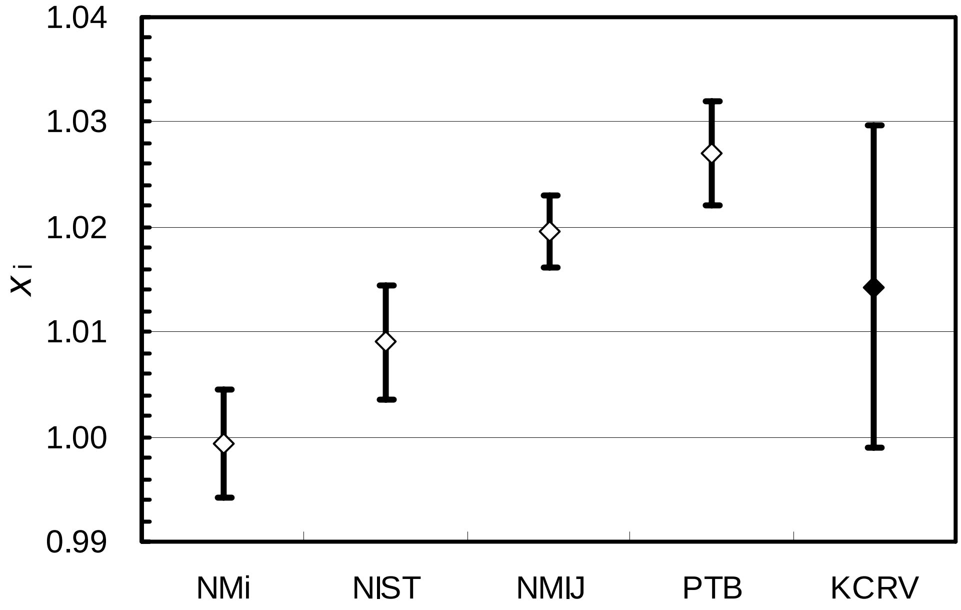

Fig. 6-1 Result of the key comparison at 2 m/s

7. Degree of Equivalence

For each participating institute, the degree of equivalence (DoE) was calculated using

$$d_i = x_i - x_{ref}. \qquad (5)$$

The results are listed in Table 7-1.

For each combination of two participating institutes, the DoE was calculated using

$$d_{i,j} = x_i - x_j. \qquad (6)$$

The expanded uncertainty was obtained using

$$U(d_{i,j}) = 2u(d_{i,j}) \qquad (7)$$

$$\text{and } u^2(d_{i,j}) = u^2(x_i) + u^2(x_j). \qquad (8)$$

The results are listed in Table 7-2 and 7-3.

Table 7-1 Degree of equivalence of each lab to KCRV

Participating Institute	20 m/s	2 m/s
NMi	-0.0048	-0.0150
NIST	-0.0033	-0.0053
NMIJ	0.0015	0.0053
PTB	0.0007	0.0127

Table 7-2 Degree of equivalence between labs and its expanded uncertainty (k = 2) at 20 m/s

Participating Institute	Degree of Equivalence and Expanded Uncertainty (k = 2)							
	NMi		NIST		NMIJ		PTB	
	d_{ij}	$U(d_{ij})$	d_{ij}	$U(d_{ij})$	d_{ij}	$U(d_{ij})$	d_{ij}	$U(d_{ij})$
NMi	-	-	0.0016	0.0080	0.0064	0.0060	0.0056	0.0060
NIST	-0.0016	0.0080	-	-	0.0048	0.0068	0.0040	0.0068
NMIJ	-0.0064	0.0060	-0.0048	0.0068	-	-	-0.0008	0.0042
PTB	-0.0056	0.0060	-0.0040	0.0068	0.0008	0.0042	-	-

Table 7-3 Degree of equivalence between labs and its expanded uncertainty (k = 2) at 2 m/s

Participating Institute	Degree of Equivalence and Expanded Uncertainty (k = 2)							
	NMi		NIST		NMIJ		PTB	
	d_{ij}	$U(d_{ij})$	d_{ij}	$U(d_{ij})$	d_{ij}	$U(d_{ij})$	d_{ij}	$U(d_{ij})$
NMi	-	-	0.0097	0.0076	0.0203	0.0062	0.0277	0.0072
NIST	-0.0097	0.0076	-	-	0.0106	0.0065	0.0180	0.0074
NMIJ	-0.0203	0.0062	-0.0106	0.0065	-	-	0.0074	0.0060
PTB	-0.0277	0.0072	-0.0180	0.0074	-0.0074	0.0060	-	-

Among the eight DoEs shown in Table 7-1, The six DoEs, except those of NMi and NIST at 20 m/s, are within the expanded uncertainty of the KCRV ($U(x_{ref})$), which is 0.0024 at 20 m/s and 0.0154 at 2 m/s with k = 2. However the DoEs of NMi and NIST at 20 m/s are smaller than the expanded uncertainties reported by each institute and listed in Table 4-1.

8. Summary and conclusion

A selected transfer standard had been circulated among the four participating institutes in eight months starting April 2005.

The CMCs of the participating institutes have been clearly validated by this key comparison.

9. References

Comité International des Poids et Mesures (CIPM), Mutual Recognition of National Measurement Standards and of Calibration and Measurement Certificates Issued by National Metrology Institutes, Paris, France, October, 1999.

Cox, M. G., The Evaluation of Key Comparison Data, Metrologia, 39, 589-595, 2002.

10. Acknowledgements

The authors would like to thank Dr. John Wright at NIST for his contribution to the arrangement and progress of this key comparison.

Appendix - Uncertainty budget of participating institutes

In this appendix, the uncertainty budget of each participating institute is presented. Each part is taken from the document submitted by the participants and has not been edited by the pilot lab.

Part 1 CCM FF K3 intercomparison on airspeed, at NMi VSL Delft, the Netherlands

Abstract

The main challenge in wind tunnel anemometry is:

1. V_{top} of the air profile is hardly ever equal to V_{avg} in the wind duct. (V_{top} is the windvelocity at the measuring point of the anemometer: the middle of the conduct and V_{avg} is the average velocity, i.e: Actual flow rate divided by the cross area of the duct)
2. Once a relationship $V_{top} = f(V_{avg})$ is determined, the anemometer under test will, depending on its geometry, affect the shape of the profile and V_{top} and a blockage correction should be applied.

Global description of the NMi anemometer testbench:

The NMi anemometer test bench consists of a test facility for atmospheric flow rates (32 - 15000 m^3/h) coupled to an open, blowing circular wind duct (200, 380, 400 ,500 or 600 mm). The flow characteristics are enhanced by means of a number of parallel 5mm hexagonal channels (honeycomb plates of 1.2 diameter, L=50 mm). The traceability is realized by means of an iterative calibration process, starting with the known actual reference volume flow rate at the position of the anemometer. The position of the measuring body is always in the centreline and plane of the free-outlet of the duct.
A feed-back control system prevents the actual flow rate from decreasing due to the flow resistance generated by the anemometer under test.

Iterative calibration process of the reference wind velocity in the duct:

1. An initial calibration of the reference anemometer is made; $V_{indicated} = f(V_{reference,1})$. In which $V_{reference,1}$ is the first estimation of V_{top}
2. The profile is determined over 4 complete axial cross- sections (positioning system,128 points per profile, resolution 0.1 mm), 8 parts of a 'pie' can be distinguished now;
3. All velocity points are corrected for density and flow rate deviations during the test;
4. Polynomial equations are developped : $V_r = f(r/R, V_{indicated})$ from r=0 up to R=duct diameter minus 5 mm;
5. The last part of the profile (5 mm to 0 mm from the pipewall) is regarded to follow Nikuradze's "power-law" .The power is chosen to that it fits the border of the polynomial of step 4 (as well as the derivative as the absolute value) and zero at r=R duct.

6. The total integral of each “1/8 pie” is calculated according to $2/8*\pi*\int_{r=0}^{r=R} V_r * r * dr$ [m^3/s] with the split function of V_r (See step 5);
7. Now, the total volume of the whole ‘pie’ has to be equal to the reference actual volume flow rate $Q_{act,avg}$ during the test run, i.e: Pie Volume * C = $Q_{act,avg}$, in which “C” is a temporary factor to adjust the initial calibration factor of the anemometer at a specific velocity.
8. The iterative process starts here: C= f(V_r) [0.1 - 50 m/s], the anemometer is corrected and steps 4 to 8 are repeated until C does not change significantly.
9. Finally, the relationship V_{top} = f (Q_{actual}) is determined.

Uncertainty budget:

Resumé

The uncertainty level of the actual flow rate is less than 0.2%. Due to the iterative calibration process, the uncertainty level in the determination of the velocity in the middle of the duct, (V_{top}) increases to 0.5% at velocities $\geq$ 1 m/s. (*k*=2)

Below 1 m/s, the uncertainty level amounts 0.5 cm/s at 1 m/s up to 3 cm/s at 0.1 m/s. (*k*=2)

Summary

The iterative calibration process of the ducts is advantageous being based upon the integral relationship of profile and volume flow as mentioned before. The initially unknown calibration factor of the small Prantl tube has no effect on the total uncertainty while the tube is used as information copier. The uncertainty sources comprise therefore only:

1. Instability of the profile during the measurements (approx. 1 hour testing for one profile);
2. Reproducibility of the delta-p sensors (0.1 Pa) used as output signal of the prantl tube;
3. The residual noise of the polynomial equation describing dP=f(v_{ref}) of the Prantl tube;
4. Uncertainty due to the assumption of the Nikuradze profile close to the wall;
5. The assumption that 8 pie parts are representative for the 3 dimensional flow profile (uncertainty due to interpolation);
6. Reproducibility of several complete calibration cycles of profiles at the same velocity;
7. Residual noise of the polynomial fit of the windtunnel factor i.e. ratio V_{top}/V_{avg} as a function of V_{avg}

Mind that flow instability due to e.g. barometric pressure, temperature, drift of blower set point is measured and therefore completely compensated for each of the 128 measuring points.

The RSS of these sources amount 0.45% so that the expanded uncertainty of the reference velocity included uncertainty of the reference flow rate (u=0.2%) yields: 0.5%

Correction for blockage effects on the virginal flow profile due to the geometry of meter under test:

Due to the limited duct size, the blockage effect of several types anemometers can not be neglected and the calibration result is corrected with a “blockage factor”. This factor is dependant on the static blockage area (the handle) and the geometry of vanes, sensors etc. The factor can be derived from calibration results of different duct diameters. Other means of determining
blockage effects are possible: i.e. with CFD, profile measurement across the surrounding area or determination of the permeability of the anemometer (especially at vane anemometers).

Uncertainty of blockage factor determination.

NMi VSL does not only work with the projected area of the object under test, though additionally uses a model that is based upon the number of blades, blade area, rounded areas (bars etc.) and sharp areas (square mounting rods, straightening vanes etc). The uncertainty of the blockage factor determination u_{block} (pneumatic blockage area) is estimated at 30% for vane anemometers.

The blockage factor of the Vane anemometer is thus calculated at 9.7 cm^2 (Blockage effect is 0.86% in the 380 mm duct with u_{block}= 0.26%)

For the Ultrasonic meter, the blockage effect is calculated with CFD and the uncertainty is estimated at 100% while no experience with similar types was available.

In the open duct as used at NMi VSL, the US meter only affects the profile due to the

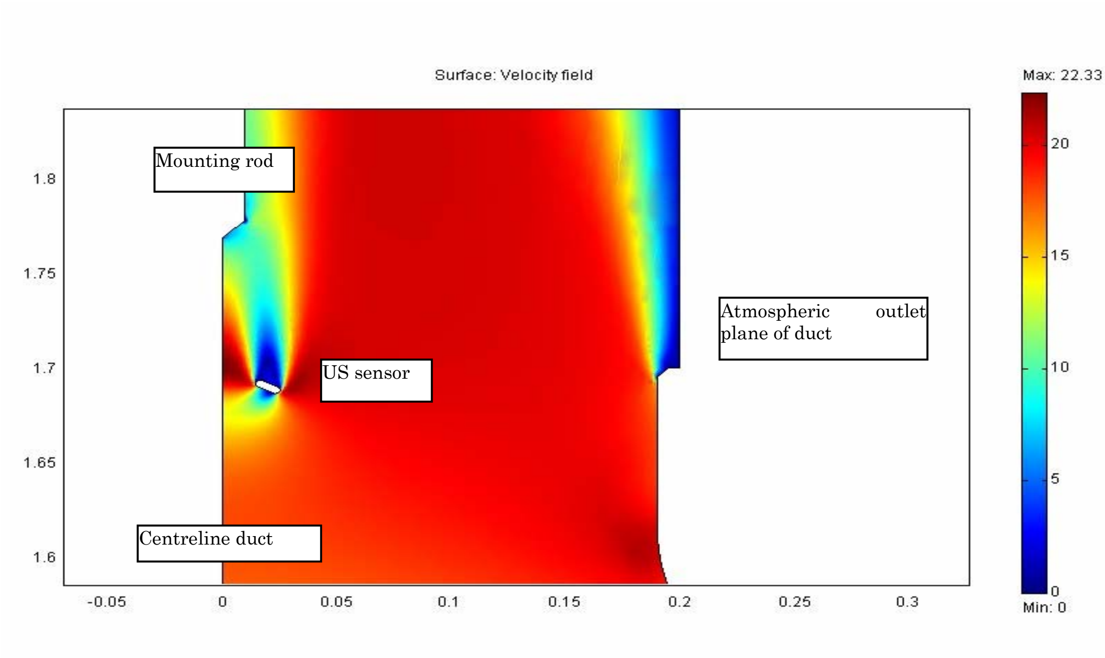

upstream us sensors. The large mounting rod and other rods do hardly affect the profile at the outlet plane.

In this exercise, the sensor plane is modelled as if it were a conical ring. In reality, one sensor is representative for 1/6 of the area of the ring and the blockage factor of the Ultrasonic anemometer is calculated accordingly at 1.4 cm^2. (Blockage effect is 0.12% in the 380 mm duct, u_{block}= 0.12%)

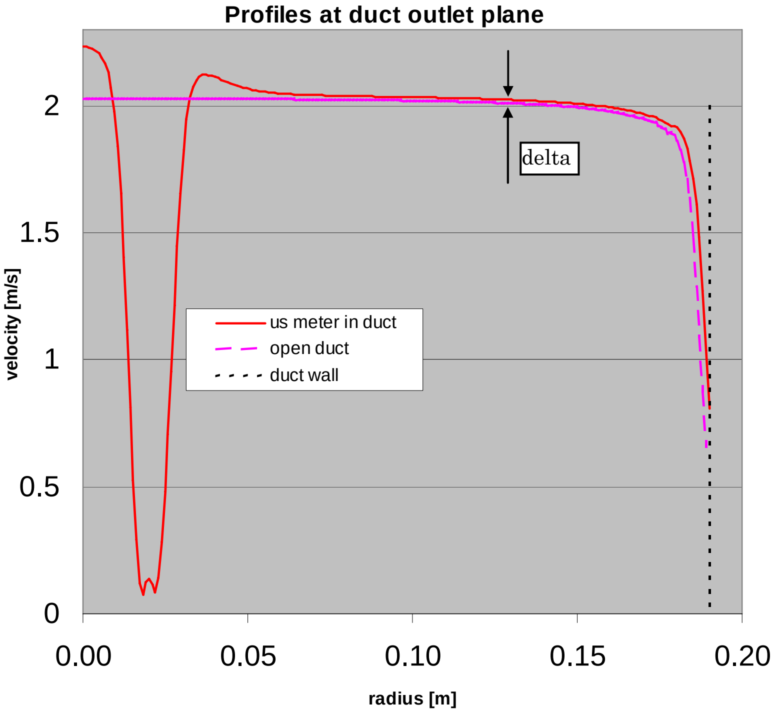

In the adjacent figure, the profiles of the virginal duct and the duct obstructed with the US anemometer is depicted at 2m/s.
At NMi VSL, the blockage factor is defined as the average percentage raise of the anemometer profile related to the virginal duct profile at the range where the tangent of the virginal profile is equal to the tangent of the anemometer profile. (See “delta”)

CMC as reported in the table of results
Finally, the repeatability of the 5 measurements (Standard deviation of the mean) is RSS added to u_{vref} and u_{block} and this resulting CMC is reported in the table. All mentioned uncertainty budgets are expressed as expanded uncertainties, coverage factor k=2

Overview Windtunnel facility at NMi VSL

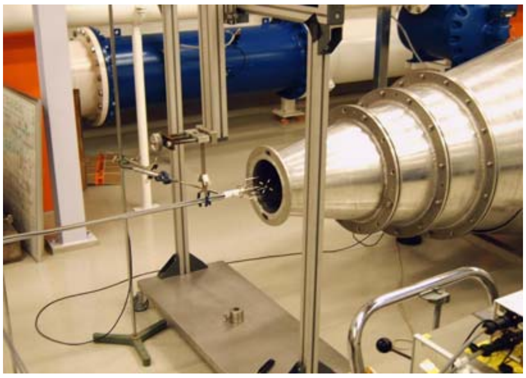

The next pictures give an overview of the intercomparison setup at NMi VSL.
In this situation, the ultrasonic meter was tested at the 200 mm duct (new laboratory Delft). At the background, two of the 5 reference meters can be seen)

The next picture gives an overview of the complete flow test rig at which the windtunnel is connected. A total of 5 reference air volume meters are used for the determination of various reference flow rates at the Meter under Test (In this case, the anemometer).

During the intercomparison, the 380 mm duct outlet was used inclusive a 20 cm long profiler-tube. This picture shows the several duct adapters at diameters 600, 500, 400 and 200 mm in Dordrecht.

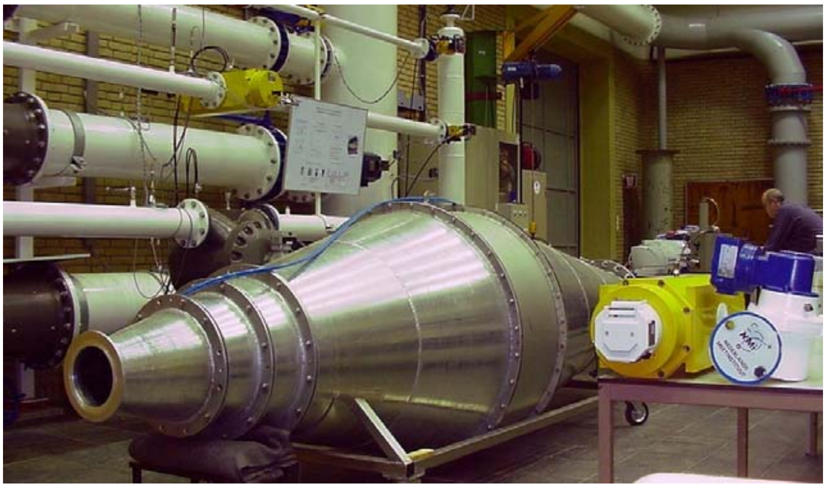

Part 2 The uncertainty of the NIST air speed standards

0.1~30 m/s, k=1		
Source of uncertainty	Type	u [m/s]
Misalignment of LDA with disk	B	0.000027
Disk radius	B	0.000068
Disk rotation rate	B	0.000085
LDA resolution	A	0.003000
LDA - Disk calibration factor	A	0.22%

At 2 m/s for k=2		
Source of uncertainty	Type	u [m/s]
Misalignment of LDA with disk	B	0.000054
Disk radius	B	0.000136
Disk rotation rate	B	0.000170
LDA resolution	A	0.006000
LDA - Disk calibration factor	A	0.008800
Expanded Uncertainty, [m/s]		0.010653
Expanded Uncertainty, [%]		0.5327

At 20 m/s for k=2		
Source of uncertainty	Type	u [m/s]
Misalignment of LDA with disk	B	0.000054
Disk radius	B	0.000136
Disk rotation rate	B	0.000170
LDA resolution	A	0.006000
LDA - Disk calibration factor	A	0.088000
Expanded Uncertainty, [m/s]		0.088205
Expanded Uncertainty, [%]		0.4410

Part 3 Uncertainty budget at PTB

The calibration has been performed by measuring the indicated air speed V_m and the reference air speed V_{ref} simultaneously in a velocity stabilized wind tunnel by means of a Laser Doppler anemometer.
The reference air speed was determined by measuring the velocity V_{LDA} at the reference measurement position taking into account the blockage effect of the transfer standard by a blockage factor k_{sonic} for the ultrasonic anemometer and k_{vane} for the vane anemometer respectively:

$V_{ref} = (k_{sonic})\ V_{LDA}$ for the ultrasonic anemometer and
$V_{ref} = (k_{vane})\ V_{LDA}$ for the vane anemometer respectively.

The uncertainty U of the calibration result V_{ref}/V_m is composed of

- $U_{ksonic,vane}$: expanded uncertainty for the blockage factor in the wind tunnel
- U_{LDA}: expanded uncertainty type B given by the calibration of the LDA
- U_{cal}: expanded uncertainty resulting from the standard deviation of the calculated mean value for the quotient V_{ref}/V_m obtained by N = 5 individual measurements according to the technical protocol and the Student factor $t_{(N-1,\ 95\%)}$.= 2,8

and has been estimated according to the following relation

$U_{sonic} = (U_{ksonic}^2 + U_{LDA}^2 + U_{cal}^2)^{0,5}$ and $U_{vane} = (U_{kvane}^2 + U_{LDA}^2 + U_{cal}^2)^{0,5}$

The expanded uncertainty for the blockage factor is based upon series of LDA measurements in the wind tunnel with and without anemometer and estimated to:

$U_{ksonic} = U_{kvane} = 0{,}22\ \%$

The semiconductor LDA has been calibrated with a rotating glass wheel serving as a velocity standard and the uncertainty has been estimated according to

$U_{LDA} = (U_{V,particle}^2 + (2s_{V,LDA})^2)^{0,5} = 0{,}10\ \%$

with $U_{V,particle} = 0{,}10\ \%$ for the uncertainty of the velocity represented by individual particles on the glass wheel and $s_{V,LDA}$ given by the standard deviation of $n \approx 2500$ LDA signal bursts from different particles passing through the LDA measuring volume at different positions.

With $U_{cal(sonic)}(2\ m/s) = 0{,}21\ \%$ and $U_{cal(sonic)}(20\ m/s) = 0{,}06\ \%$
and $U_{cal(vane)}(2\ m/s) = 0{,}44\ \%$ and $U_{cal(vane)}(20\ m/s) = 0{,}07\ \%$

one gets the overall uncertainty for the calibration result:

$U_{sonic}(2\ m/s) = 0{,}32\ \%$ and $U_{sonic}(20\ m/s) = 0{,}25\ \%$
$U_{vane}(2\ m/s) = 0{,}50\ \%$ and $U_{vane}(20\ m/s) = 0{,}25\ \%$

To get a uniform uncertainty specification for both anemometers in the wind tunnel at 2m/s and 20 m/s we declare all in all: *U* (2m/s) = 0,5 % and *U* (20 m/s) = 0,3 %

Part 4 Uncertainty budget at NMIJ

The anemometer calibration system at NMIJ consists of an LDV calibrator, an LDV transfer standard and a wind tunnel as shown in Fig. B-1. The schematic of the LVD calibrator and the wind tunnel is illustrated in Figs. B-2 and B-3.

The uncertainty budget is shown Table B-1 and B-2.

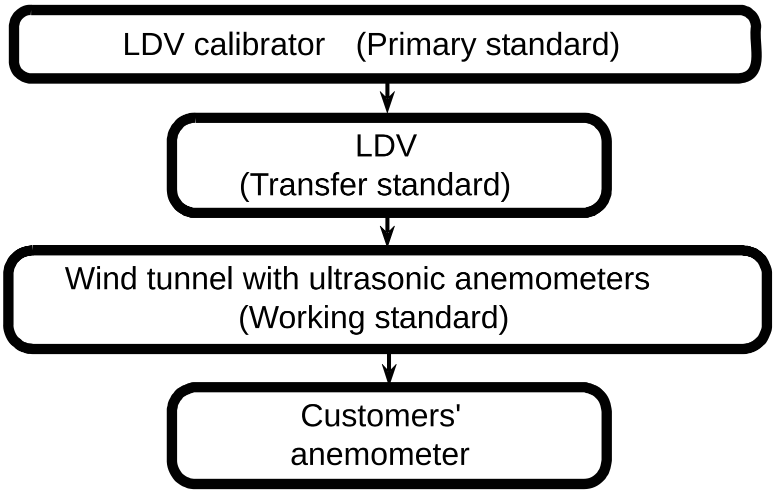

Fig. A-1 Anemometer Calibration System

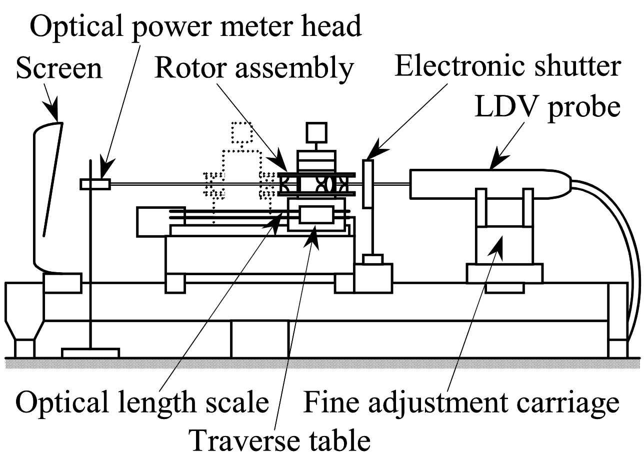

A-2 LDV Calibrator

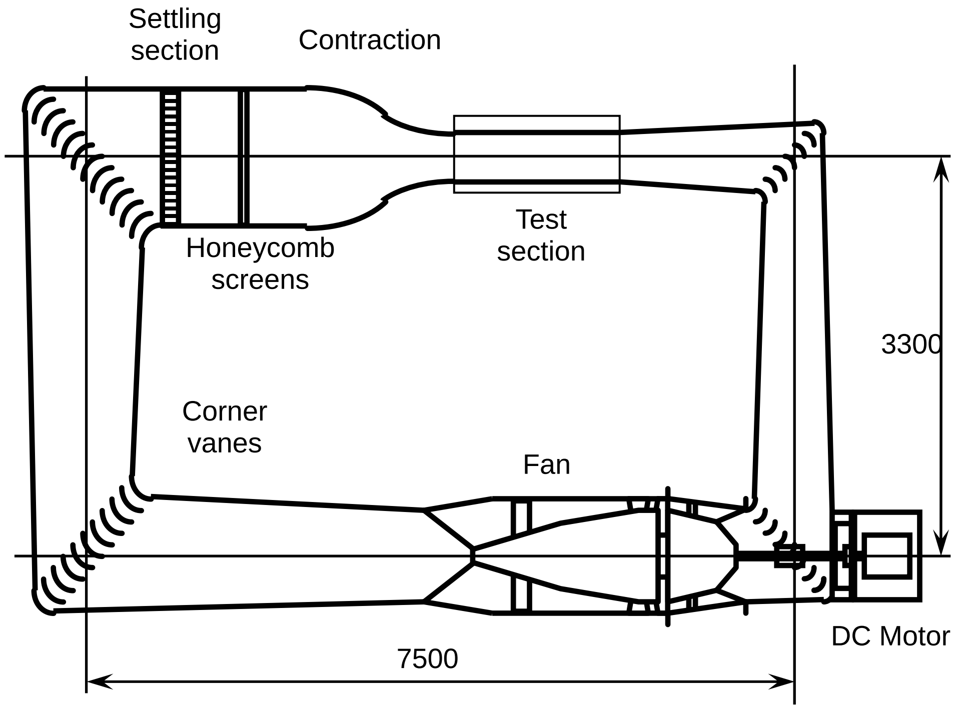

A-3 Calibration Wind Tunnel

Table A-1 Uncertainty sources and their sensitivity coefficient

Input quantity	Symbol	Uncertainty source	Sensivity coefficient	Type
Reference air speed	V_{ref}		$\lvert 1 \rvert$	
	α_{USR}	Correction factor to output value of ultrasonic reference anemometer	$\lvert 1 \rvert$	B(A)
	S_{meter}	Frontal projected area of DUT	$\left\lvert \frac{S_{\mathrm{meter}}}{S_{\mathrm{WT}} - S_{\mathrm{meter}}} \right\rvert$	A
	S_{WT}	Cross-sectional area of calibration wind tunnel	$\left\lvert \frac{-S_{\mathrm{meter}}}{S_{\mathrm{WT}} - S_{\mathrm{meter}}} \right\rvert$	A
	U^*_{USR}	Output of ultrasonic reference anemometer when DUT is installed at the test section	$\left\lvert \frac{U^*_{\mathrm{USR}}}{U^*_{\mathrm{corrctd}}} \right\rvert$	A
	U^*_{USR0}	Output of ultrasonic reference anemometer at zero air speed	$\left\lvert \frac{U^*_{\mathrm{USR0}}}{U^*_{\mathrm{corrctd}}} \right\rvert$	A
Repeatability of DUT	V_{m}		$\lvert -1 \rvert$	

Table A-2 Uncertainty budget (Symbols are defined in Table A-1)

Uncertainty sources	Air speed range												Unit
	1.3≦ ≦1.5	1.5< ≦2	2< ≦3	3< ≦5	5< ≦7	7< ≦10	10< ≦15	15< ≦20	20< ≦25	25< ≦30	30< ≦35	35< ≦40	m/s
V_{ref}	0.304	0.23	0.169	0.148	0.144	0.147	0.147	0.143	0.145	0.145	0.169	0.169	%
α_{USR}	0.303	0.229	0.169	0.148	0.143	0.147	0.147	0.143	0.145	0.145	0.169	0.169	%
S_{meter}	9.5 x10^{-03}	9.5 x10^{-03}	9.5 x10^{-03}	9.5 x10^{-03}	9.5 x10^{-03}	9.5 x10^{-03}	9.5 x10^{-03}	9.5 x10^{-03}	9.5 x10^{-03}	9.5 x10^{-03}	9.5 x10^{-03}	9.5 x10^{-03}	%
S_{WT}	9.5 x10^{-03}	9.5 x10^{-03}	9.5 x10^{-03}	9.5 x10^{-03}	9.5 x10^{-03}	9.5 x10^{-03}	9.5 x10^{-03}	9.5 x10^{-03}	9.5 x10^{-03}	9.5 x10^{-03}	9.5 x10^{-03}	9.5 x10^{-03}	%
U^*_{USR}	2.4 x10^{-04}	2.4 x10^{-04}	2.1 x10^{-04}	2.8 x10^{-04}	5.5 x10^{-04}	7.5 x10^{-04}	0.001	0.001	0.002	0.002	0.002	0.003	m/s
U^*_{USR0}	1.7 x10^{-04}	1.7 x10^{-04}	1.7 x10^{-04}	1.7 x10^{-04}	1.7 x10^{-04}	1.7 x10^{-04}	1.7 x10^{-04}	1.7 x10^{-04}	1.7 x10^{-04}	1.7 x10^{-04}	1.7 x10^{-04}	1.7 x10^{-04}	m/s
V_{m}	0.145	0.124	0.104	0.073	0.043	0.031	0.03	0.03	0.029	0.033	0.035	0.035	%
x	1	1	1	1	1	1	1	1	1	1	1	1	—
$u(x)$	0.003	0.003	0.002	0.002	0.001	0.001	0.001	0.001	0.001	0.001	0.002	0.002	—
$\frac{u(x)}{\lvert x \rvert}$	0.336	0.261	0.198	0.165	0.15	0.15	0.15	0.146	0.147	0.149	0.173	0.173	%
$\frac{U(x)}{\lvert x \rvert}$	0.673	0.523	0.397	0.331	0.3	0.299	0.299	0.292	0.294	0.298	0.346	0.346	%